Journal Pre-proofs

Wave reversal mode: a new magnetization reversal mechanism in magnetic nanotubes

Sofía Raviolo, Diana M. Arciniegas Jaimes, Noelia Bajales, Juan Escrig

Please cite this article as: S. Raviolo, M.A. Jaimes, N. Bajales, J. Escrig, Wave reversal mode: a new magnetization reversal mechanism in magnetic nanotubes, *Journal of Magnetism and Magnetic Materials* (2019), doi: https://doi.org/10.1016/j.jmmm.2019.165944

Wave reversal mode: a new magnetization reversal mechanism in magnetic nanotubes

Sofía Raviolo[1,2], Diana M. Arciniegas Jaimes[1], Noelia Bajales[1,2,*] and Juan Escrig[3,4,*]

1. CONICET, IFEG, 5000 Córdoba, Argentina.

2. Universidad Nacional de Córdoba, FaMAF, 5000 Córdoba, Argentina

3. Universidad de Santiago de Chile (USACH), Departamento de Física, 9170124 Santiago, Chile.

4. Center for the Development of Nanoscience and Nanotechnology (CEDENNA), 9170124 Santiago, Chile.

E-mail: juan.escrig@usach.cl; noelia.bajales.luna@unc.edu.ar

Abstract

We have investigated the magnetic properties of 14 nm thick and 1 μm long nickel and permalloy nanotubes with external diameters of 40 and 100 nm as a function of the angle θ at which the external magnetic field is applied. Our results show that the coercivity of 40 nm diameter nickel nanotubes follows a non-monotonic behavior from θ = 0° up to θ = 60°, while that corresponding to permalloy displays an increasing monotonic trend at the same angular range. At θ = 90°, both materials evidence a sharp drop of the coercivity to zero, indicating that the reversal mechanism has changed to a pseudo-coherent rotation. On the other hand, nickel and permalloy nanotubes with 100 nm in diameter exhibit a similar angular dependence of the coercivity, reversing their magnetization through the nucleation and propagation of vortex domain walls for angles lower than 75°. For θ = 90°, a novel striking mechanism, the wave reversal mode (W), arises. This phenomenon leads to an unusual S-type shape in the hysteresis curves at those given parameters, which is until now an effect that has not been reported for these nanostructures.

1. Introduction

Magnetic nanostructures with low dimensionality have been intensively investigated due to their potential applications in high-density magnetic memories, energy storage devices, biosensing and therapeutic uses [1-4]. In particular, magnetic nanotubes (NTs) are of great interest as multifunctional nanostructures in the field of advanced materials due to their use in a wide range of potential applications [5-10]. The magnetic properties of NTs can be controlled by varying their independent geometrical parameters such as their length, L, external diameter, d, and thickness of the tube wall, d_W (see Fig. 1a). For example, some theoretical studies [11, 12] have concluded that the relative stability of the different magnetic configurations exhibited by NTs depends strongly on their geometric and magnetic parameters. In the same way, the magnetization reversal mechanisms of NTs are strongly affected by small variations in their thickness and aspect ratio [13, 14], so the prediction of their magnetic properties is of fundamental importance for tackling the design and development of potentials applications.

In general, we can postulate three categories of magnetization reversal modes in NTs, which are widely reported in the literature [13-18] (see Fig. 1b): vortex wall (V), where spins rotate progressively via propagation of a vortex domain wall; transverse wall (T), where spins rotate progressively via propagation of a transverse domain wall, and coherent rotation (C), where all the spins (local magnetic moments) rotate simultaneously. It is worthy to note that this latter mode can suffer a variation when the magnetic moments in the caps and center of the tube are not completely parallel with each other, in which case the mode is called pseudo (or quasi)-coherent rotation (C*) [19]. It has been also found that when a magnetic field is applied parallel to the tube axis, the vortex reversal mode is the dominant magnetization reversal mechanism for tubes with radii greater than 30 nm [13]. On the other hand, different

magnetization reversal modes are observed as function of the angle in which the external magnetic field is applied, evidencing a strong angular dependence [20-22].
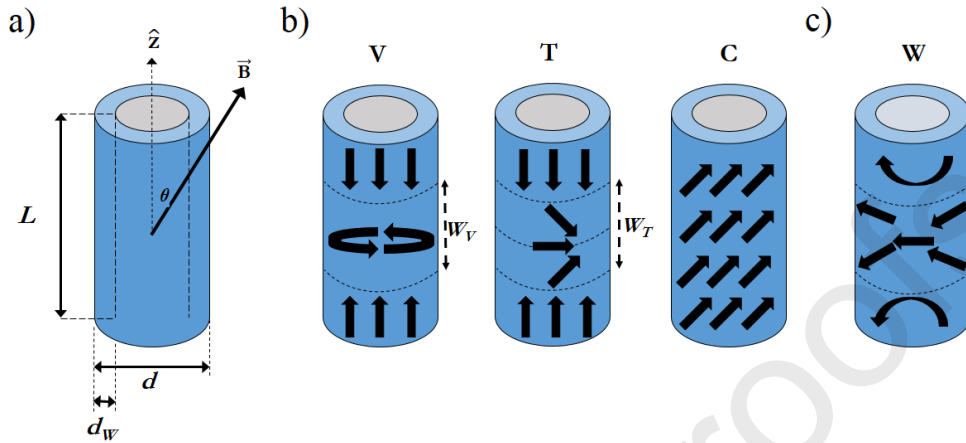

Figure 1. (a) Geometrical parameters of a magnetic nanotube. Angle between applied magnetic field and z-axis is depicted. (b) Typical magnetic switching modes in nanotubes. (c) Wave reversal mode.

In this article we perform micromagnetic simulations to investigate how the magnetic properties (coercivity, H_C, remanence, M_R, and magnetization reversal processes) of an isolated nanotube change as a function of its geometrical (diameter) and magnetic (Ni and $Ni_{80}Fe_{20}$) parameters, as well as the direction (angular dependence) in which the external magnetic field is applied. Figure 1a shows a scheme that represents the geometrical parameters of the simulated isolated nanotube and the angle θ at which an external magnetic field, $\vec{B}$, is applied. A novel and surprising magnetization reversal mechanism has been identified (see Fig. 1c), named wave reversal mode (W), which is responsible for the unusual magnetic behavior observed for isolated nanotubes of 100 nm in diameter and 1 μm in length when the magnetic field is applied perpendicular to the tube axis, a phenomenon not reported in the literature.

Figure 2 shows the reversal process of the magnetic moments of the nanotube as a function of time for this new magnetization reversal mechanism. For the initial time t_1 all magnetic moments point in the direction perpendicular to the axis of the tube, which is the direction in which the external magnetic field is applied. As the magnetic field is reduced in t_2, the magnetic moments located in the central region of the tube remain pinned in the direction perpendicular to the tube axis, while the moments in the upper half of the tube shape an "U-like" distribution, in the lower half, an "inverted U-like" arrangement, giving rise to the novel configuration of what we have called a wave (see Fig. 1c). When the magnetic field begins to increase in the opposite direction to the initial one in t_3, the magnetic moments try to align along the axis of easy magnetization of the tube, partially achieving it for the magnetic moments located on the y axis. Finally, as the intensity of the external magnetic field increases in t_4, then the magnetic moments of the tube begin to line up parallel to the external field, up to reach to the completely parallel orientation.
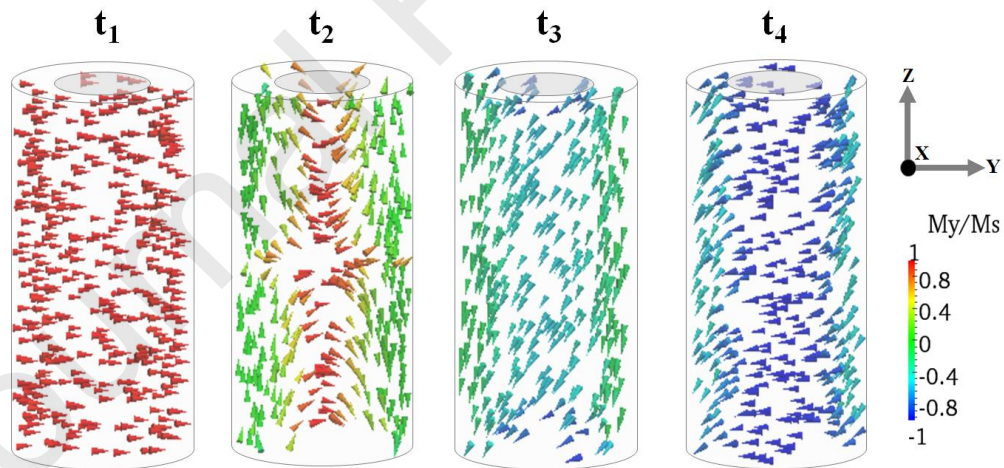

Figure 2. Snapshots of the magnetization showing the spatial behavior of the magnetic moments of the tube as a function of time when the system reverses its magnetization by means of the wave reversal mode.

4

2. Micromagnetic simulations

The magnetization dynamics in a ferromagnetic material under the action of an external magnetic field is described by the Landau-Lifshitz-Gilbert (LLG) equation [23]

$$\frac{d\vec{M}}{dt} = -\gamma \vec{M} \times \vec{H}_{eff} - \frac{\gamma \alpha}{M_s} \vec{M} \times (\vec{M} \times \vec{H}_{eff}),$$

where $\vec{M}$ is the magnetization, $\vec{H}_{eff}$ is the effective magnetic field, γ is the gyromagnetic ratio and α is the damping constant. The equation describes the precession of the magnetization around $\vec{H}_{eff}$, which exerts a torque on the magnetization proportional to the gyromagnetic ratio. The micromagnetic simulations were performed using the OOMMF software [24], which solve the LLG equation iteratively for each cell of a selected mesh and allows to monitor the temporal evolution of the system and the dynamic behavior of its magnetization.

Narrow nanotubes ($d_W = 14$ nm) of Ni and $Ni_{80}Fe_{20}$ (Py), each of $L = 1$ μm of length and external diameter of $d = 40$ and 100 nm, were simulated according to the described in the previous paragraph. We used exchange stiffness constant $A^{Ni} = 9 \times 10^{-12}$ J/m and $A^{Py} = 13 \times 10^{-12}$ J/m. The saturated magnetizations for Ni and Py were $M_s^{Ni} = 490 \times 10^3$ A/m and $M_s^{Py} = 800 \times 10^3$ A/m, respectively. The magnetocrystalline anisotropy was null because the simulated materials were considered as polycrystalline samples. In addition, we have used $\alpha = 0.5$ for both materials. For the spatial division, a cell size of $2 \times 2 \times 10$ nm^3 has been used in all cases.

3. Results and discussion

Hysteresis curves of narrow Ni nanotubes of 14 nm thickness and 1 μm long with external diameters of 40 and 100 nm are shown in Figs. 3a and 3b, respectively. Normalized magnetization (M/Ms) is depicted as a function of the angle θ at which the external magnetic

field is applied between 1.0 and −1.0 T. It is worth noting that lower applied field range 0.5 to -0.5 T is shown in order to better appreciate the differences among the different hysteresis loops.
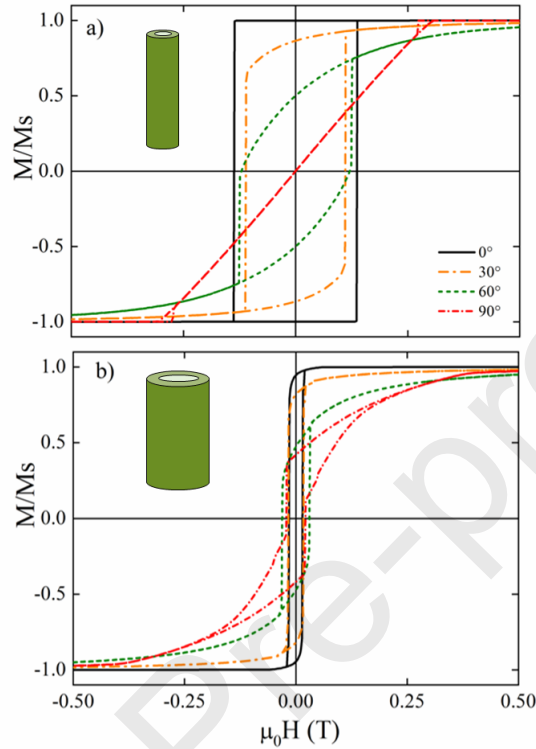

Figure 3. Normalized hysteresis curves of narrow Ni nanotubes of 14 nm thickness and 1 μm long with external diameters of (a) 40 and (b) 100 nm as a function of the angle θ at which the external magnetic field is applied.

On the one hand, the angular dependence of the magnetization for a Ni nanotube of 40 nm in diameter exhibits a noticeable squareness at θ = 0°. Coercivity at θ = 30° is smaller than those corresponding to θ = 0° and θ = 60°, suggesting a non-monotonic behavior of the coercivity from θ = 0° to θ = 60°, after which it drops to zero at θ = 90°. In addition, the remanence decreases monotonically with increasing angles. Both trends in coercivity and remanence are evidenced in Fig. 3a.

An interesting result appears when comparing these curves to those obtained for a 100 nm diameter Ni nanotube (Fig. 3b). Firstly, in this latter case, the hysteresis curves exhibit a more pronounced curved shape. Secondly, the coercivities are much lower than those obtained for a 40 nm nanotube in the angular range from $\theta = 30°$ to $\theta = 60°$. Besides coercivity at $\theta = 30°$ is slightly larger than that corresponding to $\theta = 0°$ and smaller than the one observed for $\theta = 60°$, disclosing a monotonic behavior of the coercivity from $\theta = 0°$ to $\theta = 60°$. Nonetheless, the most remarkable result is observed for the hysteresis loop at $\theta = 90°$, which exhibits a distinctive pseudo-S shape and a coercivity comparable to that obtained for $\theta = 30°$ (Fig. 3b), a pretty unexpected behavior. In fact, even though numerous theoretical and experimental studies have been carried out to investigate the static and dynamic properties of magnetic nanotubes [5-14, 20, 21], there is no evidence that this behavior had been previously observed.

In order to investigate this phenomenon in detail as well as in a comparative way with our previous work reported for a nanowire (NW) of the same material, length and diameter [22], in Fig. 4 we show snapshots of the magnetization that reveal the magnetization reversal mechanisms at $\theta = 90°$, for a 1 μm long and 100 nm diameter nanotube (Fig. 4a) and nanowire (Fig. 4b) of Ni.
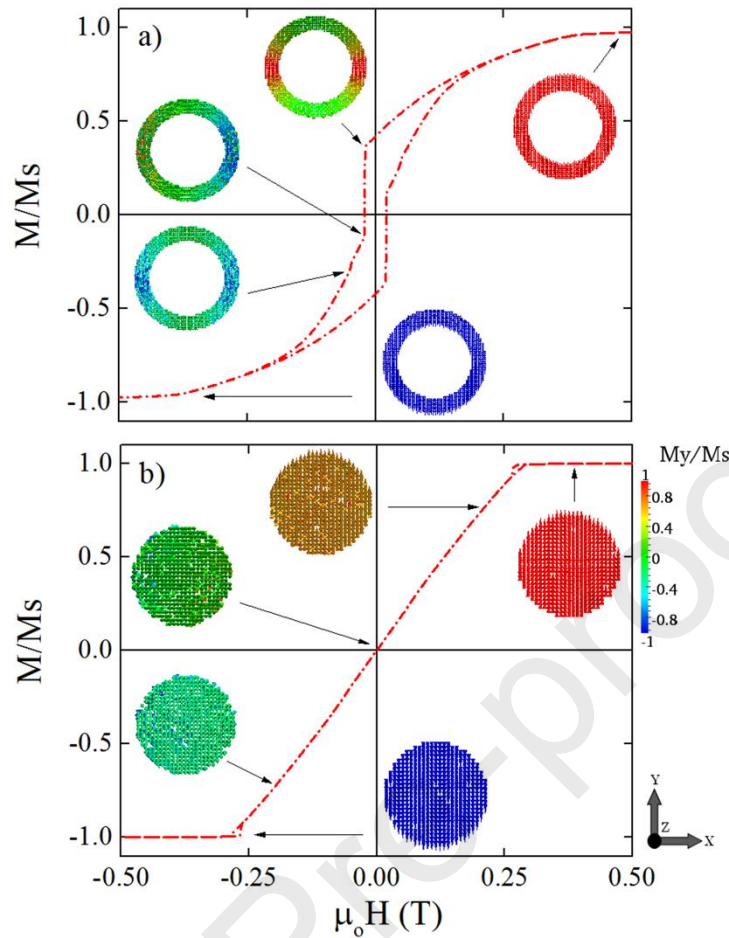
Figure 4. Normalized hysteresis curves and snapshots of cuts for θ = 90º, d = 100 nm and L = 1 μm, corresponding to different Ni nanostructures: a) 14 nm thickness NT and b) NW. The inserted images show snapshots of the magnetization of different cross sections made in the center of the (a) nanotube and (b) nanowire, indicating the evolution of reversal modes with arrows.

Fig. 4a displays the particular pseudo-S shape observed for the 100 nm diameter nanotube, where it is evinced that such nanostructure reverts its magnetization through a new reversal mechanism which we have named wave reversal mode (W), because the magnetic field generates a disturbance in the magnetic moments located in the central zone of the tube, spreading a wave towards the two ends of the tube. On the contrary, for the 100 nm Ni

8

nanowire case, we have demonstrated that if its magnetization along an unfavorable direction takes place at θ = 90°, then a small change in the magnetic field leads to an important variation in the magnetization, since the magnetic moments will be more likely perpendicular aligned to the applied field [22]. So, only a little external magnetic field is enough to modify this configuration. Such nanostructure reverses its magnetization by means of a pseudo-coherent (C*) instead of a coherent (C) rotation, due to the wire caps reverse their magnetization slightly offset from the central zone of the wire (Fig. 4b). This reversal process causes both remanence and coercivity to be zero. Likewise, this latter effect is observed for the coercivity and remanence of 40 nm Ni nanotube (Fig. 3a), advising that a pseudo-coherent rotation is also expected for this nanostructure [19].

In order to investigate if the new reversal mechanism is exclusive of Ni nanotubes or is a general phenomenon, in Fig. 5 we show the hysteresis curves for Py nanotubes with the same geometric parameters as those of Ni.
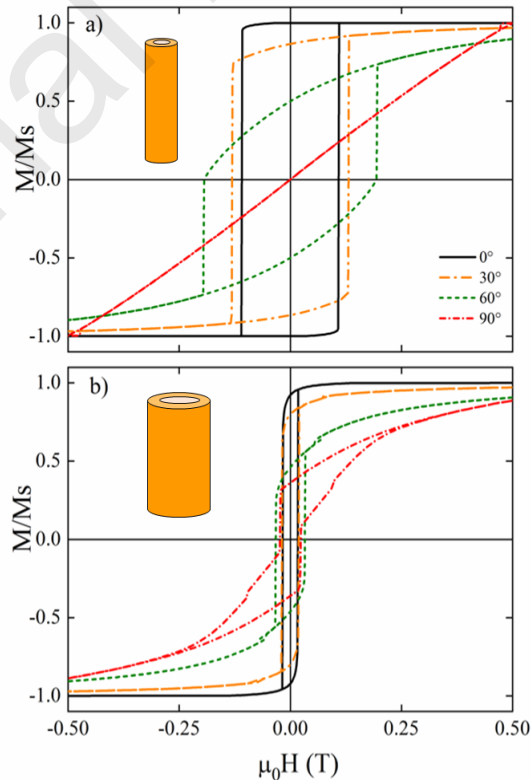
Figure 5. Normalized hysteresis curves of narrow Py nanotubes of 14 nm thickness and 1 µm long with external diameters of (a) 40 and (b) 100 nm as a function of the angle θ at which the external magnetic field is applied.

The angular dependence of the magnetization for a 40 nm diameter Py nanotube exhibits an increasing monotonic behavior of the coercivity with the angle up to 60º, after which it drops to zero at θ = 90°, while the remanence decreases monotonically with increasing angles (see Fig. 5a). Furthermore, a comparative analysis between hysteresis curves for Py nanotubes with 40 and 100 nm in diameter also shows important differences in both coercivity and remanence. For example, the squareness and coercivity for θ = 0° exhibited by the hysteresis curve of a Py nanotube of 40 nm (Fig. 5a) in diameter are clearly higher than those corresponding to the nanotube of 100 nm in diameter (Fig. 5b). Therefore, it is interesting to observe how the hysteresis curves for nanotubes of 100 nm in diameter are similar, considering the same angle, regardless of the material. In contrast, nanotubes of smaller diameters, 40 nm, exhibit a quite different behavior for the coercivity and a similar behavior for the remanence when the material varies. It is worth noting that the hysteresis curve for the Py nanotube of 100 nm in diameter measured for θ = 90º also presents an S-type shape, similar to that obtained for the Ni nanotube with the same diameter (see Figs. 3b and 5b).

So far, we have observed that the new reversal mechanism (W) appears for nanotubes of 100 nm in diameter and when the external field is applied perpendicular to the axis of the tube (θ = 90º). In order to gain insight into the magnetic properties and the magnetization reversal mechanisms of the nanotubes studied, in Fig. 6 we show the angular dependence of coercivity and remanence when θ varies between 0 and 90 degrees. It is worth to note that

the magnetization reversal mechanisms are obtained from the visualization of the magnetization snapshots for each of the simulated hysteresis curves (not shown here).
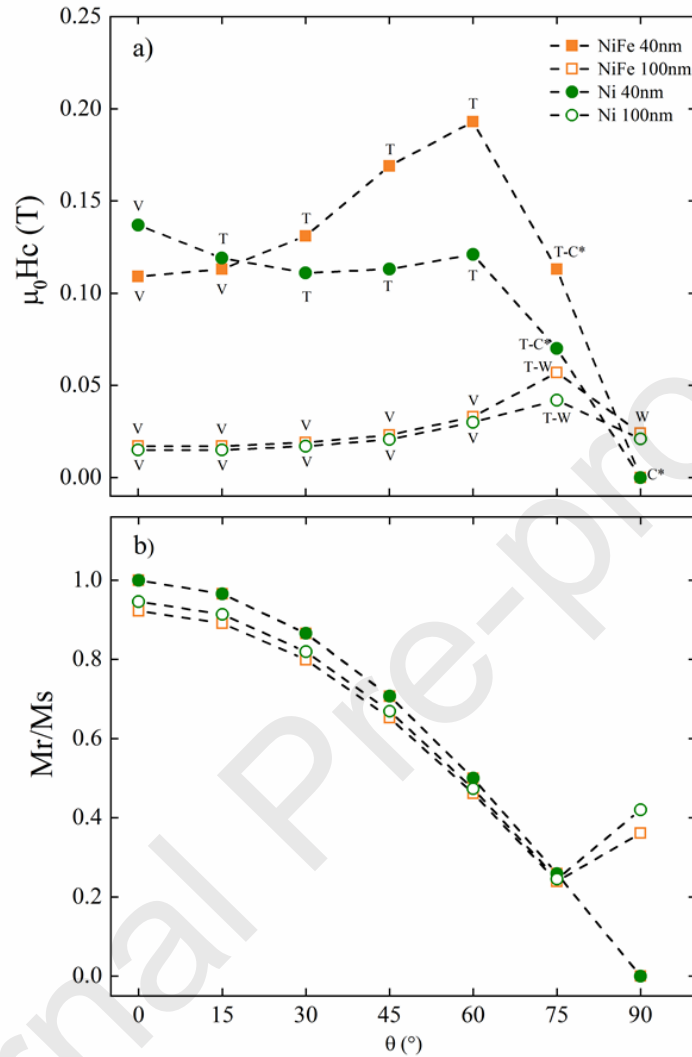

Figure 6. (a) Coercivity and (b) normalized remanence for the nanotubes studied as a function of the angle θ in which the external magnetic field is applied.

From Fig. 6a we can see that the Ni nanotube of 40 nm in diameter reverses its magnetization by propagating vortex domain walls (V) when the field is applied parallel to the tube axis (θ = 0°). For larger angles, the tube reverses its magnetization through nucleation and propagation of transverse domain walls (T) up to θ = 60º. It is interesting to remark that in this case the coercivity exhibits a non-monotonic behavior, decreasing when we move from

11

0º to 30º, after which it increases up to 60º, to decrease steeply until obtaining a zero coercivity for θ = 90º, an unequivocal signal that the reversal mechanism has changed to a pseudo-coherent rotation (C*).

On the other hand, the Py nanotubes with 40 nm in diameter reverse their magnetization by propagating vortex domain walls (V) for angles less than or equal to 15°, after which they reverse their magnetization through transverse domain walls (T), abruptly increasing its coercivity until almost doubling its value for θ = 60º. From this value, its coercivity will drop sharply again as we increase the angle θ, going through a mixed transverse-pseudo-coherent mode (T-C*) in θ = 75º, until a zero coercivity is obtained for θ = 90º, leading to a pseudo-coherent rotation (C*).

Ni and Py nanotubes with 100 nm in diameter exhibit a similar behavior for coercivity as a function of the angle θ at which the external field is applied. In both cases it is obtained that the tubes reverse their magnetization through the nucleation and propagation of vortex domain walls (V) for angles less than 75°, after which the new reversal mechanism presented in this article, the wave reversal mode (W), appears in all its fullness for θ = 90º. It is interesting to note that for all the cases investigated we obtain a complex combined magnetization reversal mechanism of nanotubes for θ = 75º.

From Fig. 6b we can notice that, regardless of the material and the diameter of the nanotubes, they all exhibit a similar behavior of the remanence as a function of the angle θ at which the external field is applied, decreasing the remanence by increasing the angle. The only exception occurs for 100 nm nanotubes when the field is applied perpendicular to its axis (θ = 90º), because the tubes reverse their magnetization by means of the new wave mechanism

(W) proposed in this article. In this way, an abrupt increase in remanence for large angles is a thorough signal that the system reverses its magnetization according to this new reversal mechanism.

It is important to note that this new mechanism of magnetization reversal (W) has not been observed in nanowires as it is evidenced in Fig. 4b [22] and, therefore, until now it is a phenomenon displayed only in nanotubes, at least for the magnetic and geometric parameters considered in this article.

Future perspectives

The focus of this article has been to introduce a new mechanism for the magnetization reversal of nanotubes that appears when they exhibit a large diameter and the magnetic field is applied perpendicular to its axis. In future work, it should be investigated how this new mechanism of magnetization reversion is exhibited by other geometric and magnetic parameters.

4. Conclusions

In conclusion, we have performed micromagnetic simulations of Ni and Py nanotubes of 14 nm thick and 1 μm long with external diameters of 40 and 100 nm as a function of the angle θ at which the external magnetic field is applied. A new striking reversal mechanism, which we have called wave reversal mode (W), has been identified. This novel phenomenon describes unusual magnetization behaviors in Ni and Py isolated nanotubes of 100 nm in diameter when the field is applied perpendicular to its axis ($\theta = 90°$). A sharp increase in remanence for large angles is an unequivocal signal that the system reverses its magnetization according to this new reversal mechanism.

Acknowledgements

References

[1] A. S. Arico, P. Bruce, B. Scrosati, J. M. Tarascon, W. Van Schalkwijk, **Nat. Mater. 4**, 366-377 (2005).

[2] D. R. Baselt, G. U. Lee, M. Natesan, S. W. Metzger, P. E. Sheehan, R. J. Colton, **Biosensors & Bioelectronics 13**, 731-739 (1998).

[3] A. Masotti, A. Caporali, **Int. J. Mol. Sci. 14**, 24619-24642 (2013).

[4] S. S. P. Parkin, M. Hayashi, L. Thomas, **Science 11**, 190-194 (2008).

[5] R. Das, J. A. Cardarelli, M. H. Phan, H. Srikanth, **J. Alloys Comp. 789**, 323-329 (2019).

[6] G. Chavez, C. H. Campos, V. A. Jimenez, C. C. Torres, C. Díaz, G. Salas, L. Guzmán, J. B. Alderete, **J. Mater. Sci. 52**, 9269-9281 (2017).

[7] D. F. Gutiérrez-Guzmán, L. I. Lizardi, J. A. Otalora, P. Landeros, **Appl. Phys. Lett. 110**, 133702 (2017).

[8] J. X. Feng, H. Xu, Y. T. Dong, X. F. Lu, Y. X. Tong, G. R. Li, **Angew. Chem. Int. Ed. 56**, 2960-2964 (2017).

[9] L. Winkless, **Materials Today 18**, 308-308 (2015).

[10] Y. X. Ye, B. Y. Geng, **Critical Reviews in Solid State and Materials Sciences 37**, 75-93 (2012).

[11] J. Escrig, P. Landeros, D. Altbir, E. E. Vogel, P. Vargas, **J. Magn. Magn. Mater. 308**, 233-237 (2007).

[12] J. Escrig, P. Landeros, D. Altbir, E. E. Vogel, **J. Magn. Magn. Mater. 310**, 2448–2450 (2007).

[13] P. Landeros, S. Allende, J. Escrig, E. Salcedo, D. Altbir, E. E. Vogel, **Appl. Phys. Lett. 90**, 102501 (2007).

[14] J. Escrig, J. Bachmann, J. Jing, M. Daub, D. Altbir, K. Nielsch, **Phys. Rev. B 77**, 214421 (2008).

[15] H. R. Liu, S. Shamaila, J. Y. Chen, R. Sharif, Q. F. Lu, X. F. Han, **Chin. Phys. Lett. 26**, 077503 (2009).

[16] M. P. Proenca, C. T. Sousa, J. Ventura, J. P. Araujo, J. Escrig, **SPIN 2**, 1250014 (2012).

[17] K. Pitzschel, J. Bachmann, J. M. Montero-Moreno, J. Escrig, D. Gorlitz, K. Nielsch, **Nanotechnology 23**, 495718 (2012).

[18] M. Sharma, B. K. Kuani, V. Veerakumar, A. Basu, Z. J. Celinski, **IEEE Trans. Magn. 50**, 2801404 (2014).

[19] D. Salazar-Aravena, J. L. Palma, J. Escrig, **Mat. Res. Express 1,** 026112 (2014).

[20] J. Escrig, M. Daub, P. Landeros, K. Nielsch, D. Altbir, **Nanotechnology 18**, 445706 (2007).

[21] O. Albrecht, R. Zierold, S. Allende, J. Escrig, C. Patzig, B. Rauschenbach, K. Nielsch, D. Görlitz, **J. Appl. Phys. 109**, 093910 (2011).

[22] S. Raviolo, F. Tejo, N. Bajales, J. Escrig, **Mater. Res. Express 5**, 015043 (2018).

[23] T. L. Gilbert, **Phys. Rev. 100**, 1243 (1955).

[24] M. J. Donahue, D. G. Porter, OOMMF User's Guide, Version 1.0, Interagency Report NISTIR 6376 (1999).

Research Highlights

- We have performed micromagnetic simulations of Ni and Py nanotubes as a function of the external magnetic field.
- A new striking reversal mechanism, which we have called wave reversal mode (W), has been identified.
- This phenomenon describes unusual behaviors in nanotubes when the field is applied perpendicular to its axis.
- A sharp increase in remanence is an unequivocal signal that the system reverses according to this mechanism.

Conflict of interest

This is an original paper and it is not being currently considered for publication elsewhere.